Volatility is rough*

Jim Gatheral
Baruch College, City University of New York
jim.gatheral@baruch.cuny.edu

Thibault Jaisson†
CMAP, École Polytechnique Paris
thibault.jaisson@polytechnique.edu

Mathieu Rosenbaum‡
École Polytechnique, CMAP
mathieu.rosenbaum@polytechnique.edu

September 30, 2017

Abstract

Estimating volatility from recent high frequency data, we revisit the question of the smoothness of the volatility process. Our main result is that log-volatility behaves essentially as a fractional Brownian motion with Hurst exponent H of order 0.1, at any reasonable time scale. This leads us to adopt the fractional stochastic volatility (FSV) model of Comte and Renault [21]. We call our model Rough FSV (RFSV) to underline that, in contrast to FSV, $H < 1/2$. We demonstrate that

*First version of the paper: 13 October 2014.

†Thibault Jaisson gratefully acknowledges financial support from the chair "Risques Financiers" of the Risk Foundation and the chair "Marchés en Mutation" of the French Banking Federation.

‡Mathieu Rosenbaum gratefully acknowledges financial support from the ERC 679836 STAQAMOF.

our RFSV model is remarkably consistent with financial time series data; one application is that it enables us to obtain improved forecasts of realized volatility. Furthermore, we find that although volatility is not a long memory process in the RFSV model, classical statistical procedures aiming at detecting volatility persistence tend to conclude the presence of long memory in data generated from it. This sheds light on why long memory of volatility has been widely accepted as a stylized fact.

Keywords: High frequency data, volatility smoothness, fractional Brownian motion, fractional Ornstein-Uhlenbeck, long memory, volatility persistence, volatility forecasting, option pricing, volatility surface.

1 Introduction

1.1 Volatility modeling

In the derivatives world, log-prices are often modeled as continuous semi-martingales. For a given asset with log-price Y_t, such a process takes the form

$$dY_t = \mu_t dt + \sigma_t dW_t,$$

where μ_t is a drift term and W_t is a one-dimensional Brownian motion. The term σ_t denotes the volatility process and is the most important ingredient of the model. In the Black-Scholes framework, the volatility function is either constant or a deterministic function of time. In Dupire's local volatility model, see [28], the local volatility $\sigma(Y_t, t)$ is a deterministic function of the underlying price and time, chosen to match observed European option prices exactly. Such a model is by definition time-inhomogeneous; its dynamics are highly unrealistic, typically generating future volatility surfaces (see Section 1.3 below) completely unlike those we observe. A corollary of this is that prices of exotic options under local volatility can be substantially off-market. On the other hand, in so-called stochastic volatility models, the volatility σ_t is modeled as a continuous Brownian semi-martingale. Notable amongst such stochastic volatility models are the Hull and White model [41], the Heston model [40], and the SABR model [39]. Whilst stochastic volatility dynamics are more realistic than local volatility dynamics, generated option prices are not consistent with observed European option prices. We refer to [33] and

[46] for more detailed reviews of the different approaches to volatility modeling. More recent market practice is to use local-stochastic-volatility (LSV) models which both fit the market exactly and generate reasonable dynamics.

Consistent with our focus on derivatives, our goal in this work is to replicate features of the observed time series of volatility over time scales from one day to ten years say. Indeed, volatility modeling can probably only be relevant at time scales of order one day or more. Below this, at the sub-second time scale for example, it is not even clear what the meaning of volatility is (independently of a specific model). Nevertheless, in order to get accurate volatility measurements, we will rely on high frequency methods in our estimation procedures.

1.2 Fractional volatility

In terms of the smoothness of the volatility process, the preceding models offer two possibilities: very regular sample paths in the case of Black-Scholes, and volatility trajectories with regularity close to that of Brownian motion for the local and stochastic volatility models. Starting from the stylized fact that volatility is a long memory process, various authors have proposed models that allow for a wider range of regularity for the volatility. In a pioneering paper, Comte and Renault [21] proposed to model log-volatility using fractional Brownian motion (fBm for short), ensuring long memory by choosing the Hurst parameter $H > 1/2$. A large literature has subsequently developed around such fractional volatility models, for example [16, 20, 51].

The fBm $(W_t^H)_{t\in\mathbb{R}}$ with Hurst parameter $H \in (0,1)$, introduced in [43], is a centered self-similar Gaussian process with stationary increments satisfying for any $t \in \mathbb{R}$, $\Delta \geq 0$, $q > 0$:

$$\mathbb{E}[|W_{t+\Delta}^H - W_t^H|^q] = K_q \Delta^{qH}, \tag{1.1}$$

with K_q the moment of order q of the absolute value of a standard Gaussian variable. For $H = 1/2$, we retrieve the classical Brownian motion. The sample paths of W^H are Hölder-continuous with exponent r, for any $r < H$[1].

[1] Actually H corresponds to the regularity of the process in a more accurate way: in terms of Besov smoothness spaces, see Section 2.1.

Finally, when $H > 1/2$, the increments of the fBm are positively correlated and exhibit long memory in the sense that

$$\sum_{k=0}^{+\infty} \mathrm{Cov}[W_1^H, W_k^H - W_{k-1}^H] = +\infty.$$

Indeed, $\mathrm{Cov}[W_1^H, W_k^H - W_{k-1}^H]$ is of order k^{2H-2} as $k \to \infty$. Note that in the case of the fBm, there is a one to one correspondence between regularity and long memory through the Hurst parameter H.

As mentioned earlier, the long memory property of the volatility process has been widely accepted as a stylized fact since the seminal analyses of Ding, Granger and Engle [26], Andersen and Bollerslev [2] and Andersen et al. [4]. Initially, it appears that the term *long memory* referred to the slow decay of the autocorrelation function (of absolute returns for example), anything slower than exponential. Over time however, it seems that this term has acquired the more precise meaning that the autocorrelation function is not integrable, see [10], and even more precisely that it decays as a power-law with exponent less than 1. Much of the more recent literature, for example [9, 15, 17], assumes long memory in volatility in this more technical sense. Indeed, meaningful results can probably only be obtained under such a specification, since it is not possible to estimate the asymptotic behavior of the covariance function without assuming a specific form. Nevertheless, analyses such as that of Andersen et al. [4] use data that predate the advent of high-frequency electronic trading, and the evidence for long memory has never been sufficient to satisfy remaining doubters such as Mikosch and Stărică in [45]. To quote Rama Cont in [22]:

> ... the econometric debate on the short range or long range nature of dependence in volatility still goes on (and may probably never be resolved)...

In the spirit of the above quote, in our view, the question as to whether the volatility time series exhibits long memory (in a technical sense) or not is not a very useful or fruitful one. Indeed we believe that in practice, the concept of long memory is too fragile to be applicable to an analysis involving ultra high frequency data (for example any seasonality may give rise to spurious long memory). Therefore we do not focus on long memory in this work. Still, we do show that the autocorrelation function of volatility does not behave as a power law, at least at usual time scales of observation. In particular, we are able to provide explicit expressions enabling us to analyze thoroughly the dependence structure of the volatility process.

1.3 The shape of the implied volatility surface

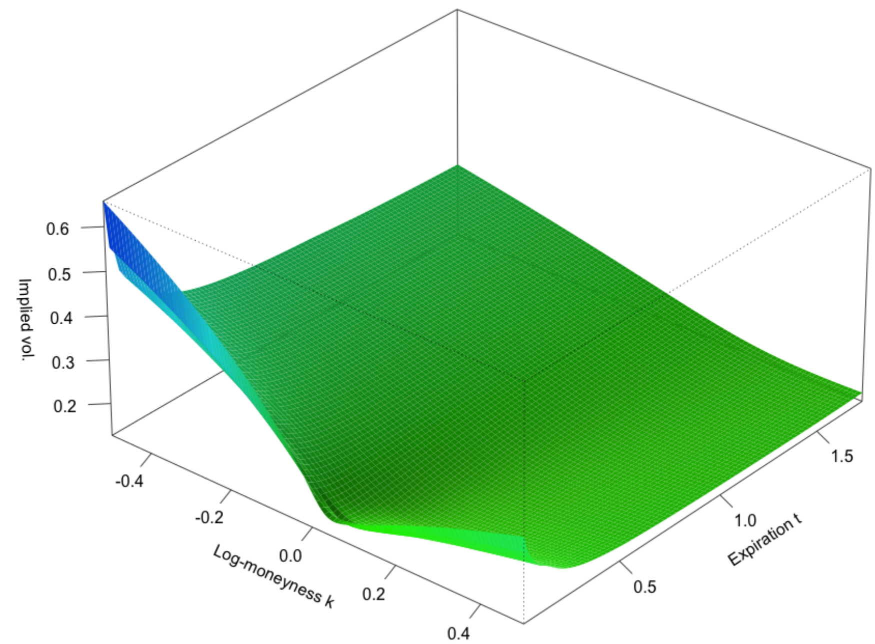

Figure 1.1: The S&P volatility surface as of June 20, 2013.

As is well-known, the implied volatility $\sigma_{\mathrm{BS}}(k,\tau)$ of an option (with log-moneyness k and time to expiration τ) is the value of the volatility parameter in the Black-Scholes formula required to match the market price of that option. Plotting implied volatility as a function of strike price and time to expiry generates the *volatility surface*, explored in detail in, for example, [33]. A typical such volatility surface generated from a "stochastic volatility inspired" (SVI) [34] fit to closing SPX option prices as of June 20, 2013[2] is shown in Figure 1.1. It is a stylized fact that, at least in equity markets, although the level and orientation of the volatility surface do change over time, the general overall shape of the volatility surface does not change, at least to a first approximation. This suggests that it is desirable to model volatility as a time-homogenous process, *i.e.* a process whose parameters are independent of price and time.

However, conventional time-homogenous models of volatility such as the Hull and White, Heston, and SABR models do not fit the volatility surface. In particular, as shown in Figure 1.2, the observed term structure of at-the-money ($k = 0$) volatility skew

$$\psi(\tau) := \left| \frac{\partial}{\partial k} \sigma_{\mathrm{BS}}(k, \tau) \right|_{k=0}$$

is well-approximated by a power-law function of time to expiry τ. In contrast, conventional stochastic volatility models generate a term structure of at-the-money (ATM) skew that is *constant* for small τ and behaves as a sum of decaying exponentials for larger τ.

[2] Closing prices of SPX options for all available strikes and expirations as of June 20, 2013 were sourced from OptionMetrics (www.optionmetrics.com) via Wharton Research Data Services (WRDS).

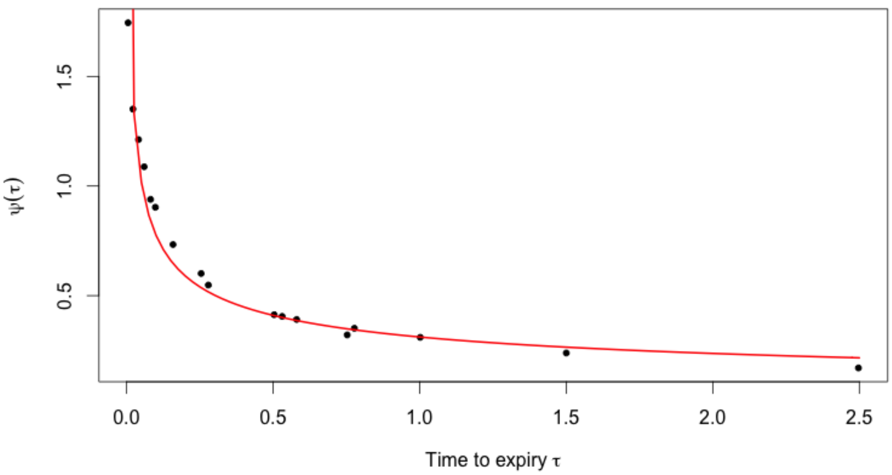

Figure 1.2: The black dots are non-parametric estimates of the S&P ATM volatility skews as of June 20, 2013; the red curve is the power-law fit $\psi(\tau) = A\,\tau^{-0.4}$.

In Section 3.3 of [32], as an example of the application of his martingale expansion, Fukasawa shows that a stochastic volatility model where the volatility is driven by fractional Brownian motion with Hurst exponent H generates an ATM volatility skew of the form $\psi(\tau) \sim \tau^{H-1/2}$, at least for small τ. This is interesting in and of itself in that it provides a counterexample to the widespread belief that the explosion of the volatility smile as $\tau \to 0$ (as clearly seen in Figures 1.1 and 1.2) implies the presence of jumps [14]. The main point here is that for a model of the sort analyzed by Fukasawa to generate a volatility surface with a reasonable shape, we would need to have a value of H close to zero. As we will see in Section 2, our empirical estimates of H from time series data are in fact very small.

The volatility model that we will specify in Section 3.1, driven by fBm with $H < 1/2$, therefore has the potential to be not only consistent with the empirically observed properties of the volatility time series but also consistent with the shape of the volatility surface. In this paper, we focus on the modeling of the volatility time series. A more detailed analysis of the consistency of our model with option prices is provided in [7].

1.4 Main results and organization of the paper

In Section 2, we report our estimates of the smoothness of the log-volatility for selected assets. This smoothness parameter lies systematically between 0.08 and 0.2 (in the sense of Hölder regularity for example). Furthermore, we find that increments of the log-volatility are approximately normally distributed and that their moments enjoy a remarkable monofractal scaling property. This leads us to model the log of volatility using a fBm with Hurst parameter $H < 1/2$ in Section 3. Specifically we adopt the fractional stochastic volatility (FSV) model of Comte and Renault [21]. We call our model Rough FSV (RSFV) to underline that, in contrast to FSV, we take $H < 1/2$. We also show in the same section that the RFSV model is remarkably consistent with volatility time series data. The issue of volatility persistence is considered through the lens of the RFSV model in Section 4. Our main finding is that although the RFSV model does not have any long memory property, classical statistical procedures aiming at detecting volatility persistence tend to conclude the presence of long memory in data generated from it. This sheds new light on the supposed long memory in the volatility of financial data. In Section 5, we finally apply our model to volatility forecasting. In particular, we show that RFSV volatility forecasts outperform conventional AR and HAR volatility forecasts. Some proofs are relegated to the appendix.

2 Smoothness of the volatility: empirical results

In this section we report estimates of the smoothness of the volatility process for four assets:

- The DAX and Bund futures contracts, for which we estimate integrated variance directly from high frequency data using an estimator based on the model with uncertainty zones, see [49, 50]. This model enables us to safely use all the ultra high frequency price data in order to perform our estimation, and thus to obtain accurate estimates over short time windows.

- The S&P and NASDAQ indices, for which we use precomputed realized variance estimates from the Oxford-Man Institute of Quantitative Finance Realized Library[3].

2.1 Estimating the smoothness of the volatility process

Let us first pretend that we have access to discrete observations of the volatility process, on a time grid with mesh Δ on $[0,T]$: $\sigma_0,\ \sigma_\Delta,\dots,\sigma_{k\Delta},\dots,$ $k \in \{0, \lfloor T/\Delta \rfloor\}$. Set $N = \lfloor T/\Delta \rfloor$, then for $q \geq 0$, we define

$$m(q,\Delta) = \frac{1}{N}\sum_{k=1}^{N} |\log(\sigma_{k\Delta}) - \log(\sigma_{(k-1)\Delta})|^q.$$

In the spirit of [53], our main assumption is that for some $s_q > 0$ and $b_q > 0$, as Δ tends to zero,

$$N^{qs_q} m(q,\Delta) \to b_q. \tag{2.1}$$

Under additional technical conditions, Equation (2.1) essentially says that the volatility process belongs to the Besov smoothness space $\mathcal{B}^{s_q}_{q,\infty}$ and does not belong to $\mathcal{B}^{s'_q}_{q,\infty}$, for $s'_q > s_q$, see [52]. Hence s_q can really be viewed as the regularity of the volatility when measured in l_q norm. In particular, functions in $\mathcal{B}^{s}_{q,\infty}$ for every $q > 0$ enjoy the Hölder property with parameter h for any $h < s$. For example, if $\log(\sigma_t)$ is a fBm with Hurst parameter H, then for any $q \geq 0$, Equation (2.1) holds in probability with $s_q = H$ and it can be shown that the sample paths of the process indeed belong to $\mathcal{B}^{H}_{q,\infty}$ almost surely. Assuming the increments of the log-volatility process are stationary and that a law of large numbers can be applied, $m(q,\Delta)$ can also be seen as the empirical counterpart of

$$\mathbb{E}[|\log(\sigma_\Delta) - \log(\sigma_0)|^q].$$

Of course the volatility process is not directly observable, and an exact computation of $m(q,\Delta)$ is not possible in practice. We must therefore proxy spot volatility values by appropriate estimated values. Since the minimal Δ will

[3] http://realized.oxford-man.ox.ac.uk/data/download. The Oxford-Man Institute's Realized Library contains a selection of daily non-parametric estimates of volatility of financial assets, including realized variance (rv) and realized kernel (rk) estimates. A selection of such estimators is described and their performances compared in, for example, [35].

be equal to one day in the sequel, we proxy the (true) spot volatility daily at a fixed given time of the day (11 am for example). Two daily spot volatility proxies will be considered:

- For our ultra high frequency intraday data (DAX future contracts and Bund future contracts[4], 1248 days from 13/05/2010 to 01/08/2014[5]), we use the estimator of the integrated variance from 10 am to 11 am London time obtained from the model with uncertainty zones, see [49, 50]. After renormalization, the resulting estimates of integrated variance over very short time intervals can be considered as good proxies for the unobservable spot variance. In particular, the one hour long window on which they are computed is small compared to the extra day time scales that will be of interest here.

- For the S&P and NASDAQ indices[6], we proxy daily spot variances by daily realized variance estimates from the Oxford-Man Institute of Quantitative Finance Realized Library (3,540 trading days from January 3, 2000 to March 31, 2014). Since these estimates of integrated variance are for the whole trading day, we expect estimates of the smoothness of the volatility process to be biased upwards, integration being a regularizing operation. We compute the extent of this bias by simulation in Section 3.4 and more quantitatively in Appendix C.

In the following, we retain the notation $m(q, \Delta)$ with the understanding that we are only proxying the (true) spot volatility as explained above. We now proceed to estimate the smoothness parameter s_q for each q by computing the $m(q, \Delta)$ for different values of Δ and regressing $\log m(q, \Delta)$ against $\log \Delta$. Note that for a given Δ, several $m(q, \Delta)$ can be computed depending on the starting point. Our final measure of $m(q, \Delta)$ is the average of these values.

2.2 DAX and Bund futures contracts

DAX and Bund futures are amongst the most liquid assets in the world and moreover, the model with uncertainty zones used to estimate volatility is

[4]For every day, we only consider the future contract corresponding to the most liquid maturity.

[5]Data kindly provided by QuantHouse EUROPE/ASIA, http://www.quanthouse.com.

[6]And also the CAC40, Nikkei and FTSE indices in some specific parts of the paper.

known to apply well to them, see [24]. So we can be confident in the reliability of our volatility proxy. Nevertheless, as an extra check, we will confirm the quality of our volatility proxy by Monte Carlo simulation in Section 3.4.

Plots of $\log m(q, \Delta)$ vs $\log \Delta$ for different values of q are displayed for the DAX in Figure 2.1, and for the Bund in Figure 2.2.

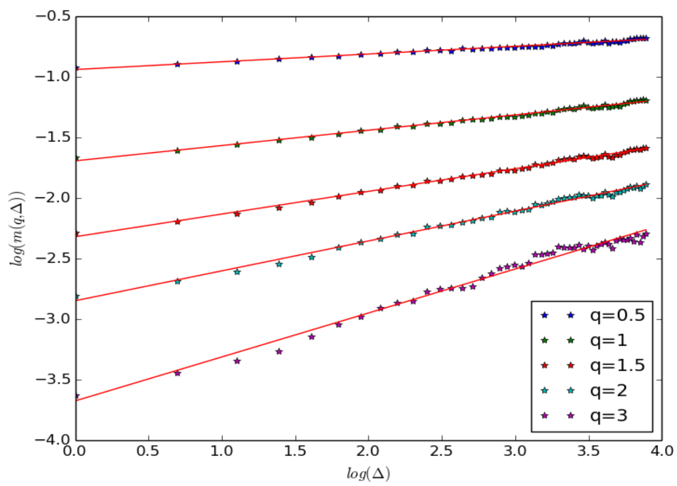

Figure 2.1: $\log m(q, \Delta)$ as a function of $\log \Delta$, DAX.

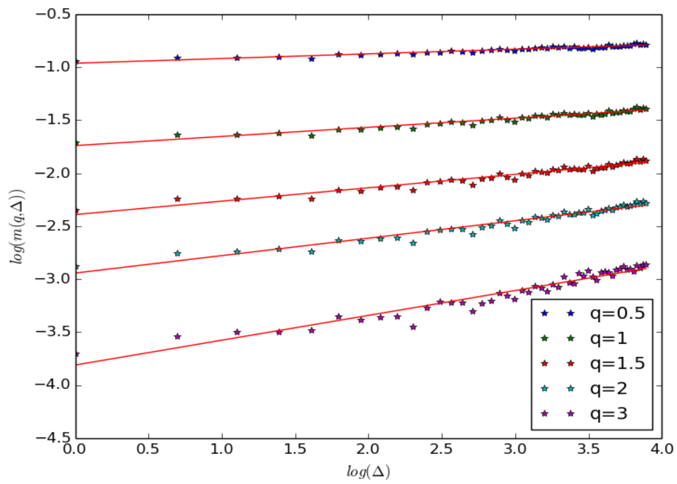

Figure 2.2: $\log m(q, \Delta)$ as a function of $\log \Delta$, Bund.

For both DAX and Bund, for a given q, the points essentially lie on a straight line. Under stationarity assumptions, this implies that the log-volatility increments enjoy the following scaling property in expectation:

$$\mathbb{E}[|\log(\sigma_\Delta) - \log(\sigma_0)|^q] = b_q \Delta^{\zeta_q},$$

where $\zeta_q = q s_q > 0$ is the slope of the line associated to q. Moreover, the smoothness parameter s_q does not seem to depend on q. Indeed, plotting ζ_q against q, we obtain that $\zeta_q \sim H\, q$ with H equal to 0.125 for the DAX and to 0.082 for the Bund, see Figure 2.3.

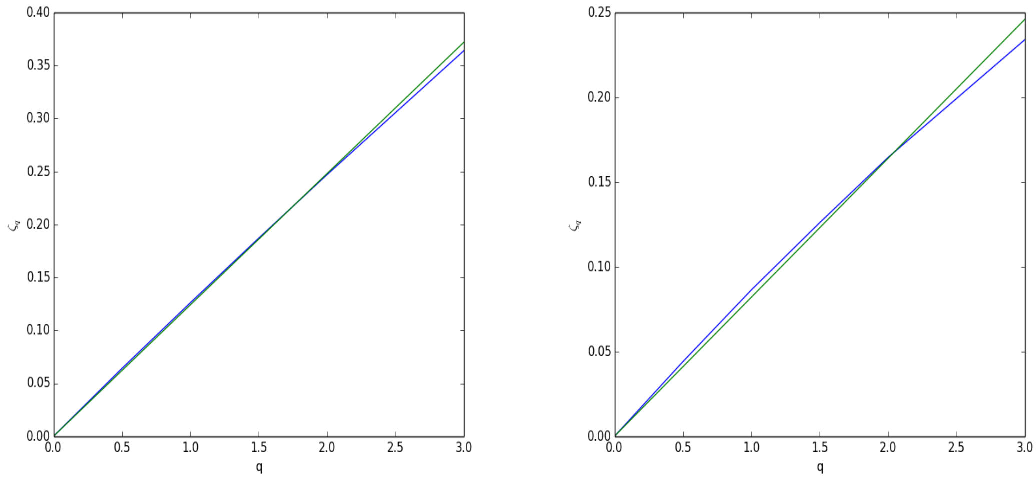

Figure 2.3: ζ_q (blue) and $0.125 \times q$ (green), DAX (left); ζ_q (blue) and $0.082 \times q$ (green), Bund (right).

We remark that the graphs for ζ_q are actually very slightly concave. However, we observe the same small concavity effect when we replace the log-volatility by simulations of a fBm with the same number of points. We conclude that this effect relates to finite sample size and is thus not significant.

2.3 S&P and NASDAQ indices

We report in Figure 2.4 and Figure 2.5 similar results for the S&P and NASDAQ indices. The variance proxies used here are the precomputed 5-minute realized variance estimates for the whole trading day made publicly available by the Oxford-Man Institute of Quantitative Finance.

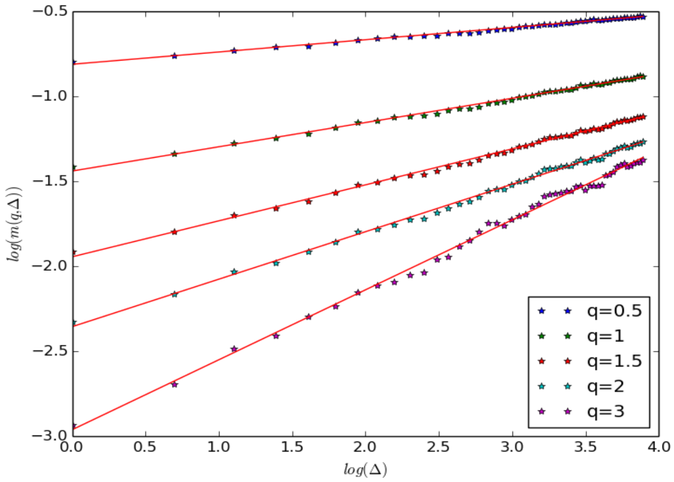

Figure 2.4: $\log m(q, \Delta)$ as a function of $\log \Delta$, S&P.

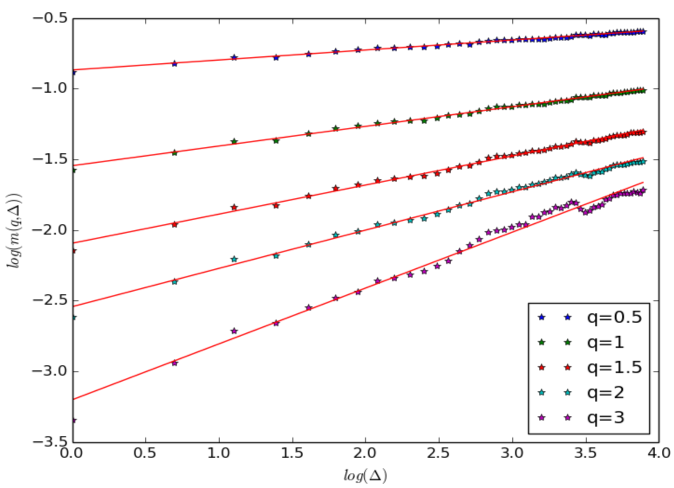

Figure 2.5: $\log m(q, \Delta)$ as a function of $\log(\Delta)$, NASDAQ.

We observe the same scaling property for the S&P and NASDAQ indices as we observed for DAX and Bund futures and again, the s_q do not depend on

q. However, the estimated smoothnesses are slightly higher here: $H = 0.142$ for the S&P and $H = 0.139$ for the NASDAQ, see Figure 2.6.

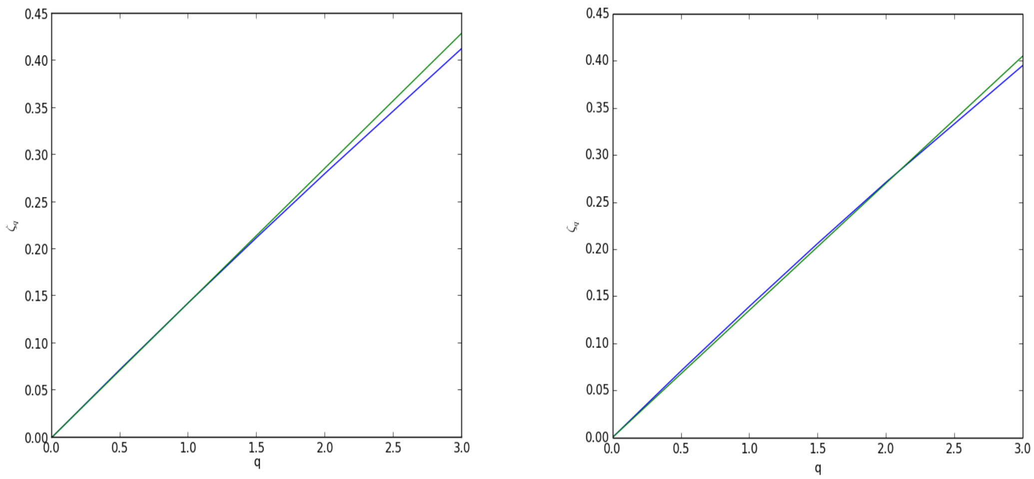

Figure 2.6: ζ_q (blue) and $0.142 \times q$ (green), S&P (left); ζ_q (blue) and $0.139 \times q$ (green), NASDAQ (right).

Once again, we do expect these smoothness estimates to be biased high because we are using whole-day realized variance estimates, as explained earlier in Section 2. Finally, we remark that as for DAX and Bund futures, the graphs for ζ_q are slightly concave.

2.4 Other indices

Repeating the analysis of Section 2.3 for each index in the Oxford-Man dataset, we find the $m(q, \Delta)$ present a universal scaling behavior. For each index and for $q = 0.5,\ 1,\ 1.5,\ 2,\ 3$, by doing a linear regression of $\log(m(q, \Delta))$ on $\log(\Delta)$ for $\Delta = 1, ..., 30$, we obtain estimates of ζ_q that we summarize in Table B.1 in the appendix.

2.5 Distribution of the increments of the log-volatility

Having established that all our underlying assets exhibit essentially the same scaling behavior[7], we focus in the rest of the paper only on the S&P index, unless specified otherwise. That the distribution of increments of log-volatility is close to Gaussian is a well-established stylized fact reported for example in the papers [3] and [4] of Andersen et al. Looking now at the histograms of the increments of the log-volatility in Figure 2.7, with the fitted normal density superimposed in red, we see that, for any Δ, the empirical distribution of log-volatility increments is verified as being close to Gaussian. More impressive still is that rescaling the 1-day fit of the normal density by Δ^H generates (blue dashed) curves that are very close to the red fits of the normal density, consistent with the observed scaling.

[7]We have also verified that this scaling relationship holds for Crude Oil and Gold futures, with similar smoothness estimates.

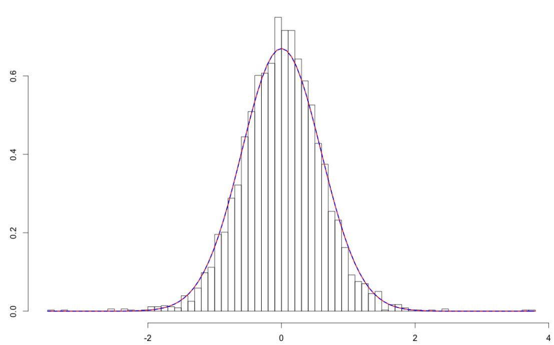

(a) $\Delta = 1$ day

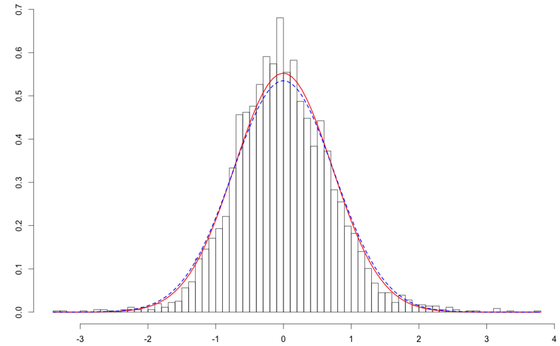

(b) $\Delta = 5$ days

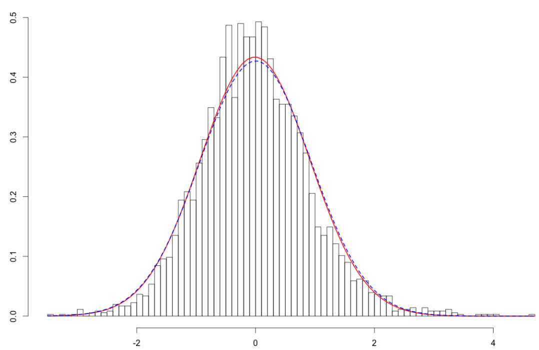

(c) $\Delta = 25$ days

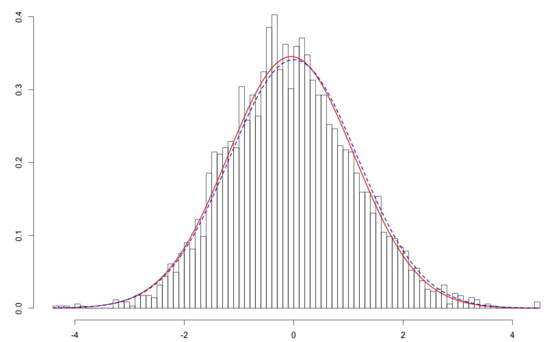

(d) $\Delta = 125$ days

Figure 2.7: Histograms for various lags Δ of the (overlapping) increments $\log \sigma_{t+\Delta} - \log \sigma_t$ of the S&P log-volatility; normal fits in red; normal fit for $\Delta = 1$ day rescaled by Δ^H in blue.

The slight deviations from the Normal distribution observed in Figure 2.7 are again consistent with the computation of the empirical distribution of the increments of a fractional Brownian motion on a similar number of points.

2.6 Does H vary over time?

In order to check whether our estimations of H depends on the time interval, we split the Oxford-Man realized variance dataset into two halves and reestimate H for each half separately. The results are presented in Table B.2 in the appendix. We note that although the estimated H all lie between 0.06

and 0.20, they seem to be higher in the second period which includes the financial crisis.

3 A simple model compatible with the empirical scaling of the volatility

In this section, we specify the Rough FSV model and demonstrate that it reproduces the empirical facts presented in Section 2.

3.1 Specification of the RFSV model

In the previous section, we showed that, empirically, the increments of the log-volatility of various assets enjoy a scaling property with constant smoothness parameter and that their distribution is close to Gaussian. This naturally suggests the simple model:

$$\log \sigma_{t+\Delta} - \log \sigma_t = \nu \left(W^H_{t+\Delta} - W^H_t \right), \tag{3.1}$$

where W^H is a fractional Brownian motion with Hurst parameter equal to the measured smoothness of the volatility and ν is a positive constant. We may of course write (3.1) under the form

$$\sigma_t = \sigma \exp(\nu \, W^H_t), \tag{3.2}$$

where σ is another positive constant.

However this model is not stationary, stationarity being desirable both for mathematical tractability and also to ensure reasonableness of the model at very large times. This leads us to impose stationarity by modeling the log-volatility as a fractional Ornstein-Uhlenbeck process with a very long reversion time scale.

A stationary fractional Ornstein-Uhlenbeck process (X_t) is defined as the stationary solution of the stochastic differential equation

$$dX_t = \nu \, dW^H_t - \alpha \, (X_t - m) dt,$$

where $m \in \mathbb{R}$ and ν and α are positive parameters, see [16]. As for usual Ornstein-Uhlenbeck processes, there is an explicit form for the solution which is given by

$$X_t = \nu \int_{-\infty}^{t} e^{-\alpha(t-s)} dW_t^H + m. \tag{3.3}$$

Here the stochastic integral with respect to fBm is simply a pathwise Riemann-Stieltjes integral, see again [16].

We thus arrive at the final specification of our Rough Fractional Stochastic Volatility (RFSV) model for the volatility on the time interval of interest $[0, T]$:

$$\sigma_t = \exp(X_t),\ t \in [0, T], \tag{3.4}$$

where (X_t) satisfies Equation (3.3) for some $\nu > 0$, $\alpha > 0$, $m \in \mathbb{R}$ and $H < 1/2$ the measured smoothness of the volatility. This model provides a very parsimonious description of the volatility process with only four parameters (and in practice only three, see below). Moreover, statistical inference methods for fractional Brownian motion and fractional Ornstein-Uhlenbeck process are well known, see [13, 19, 42].

Such a model is indeed stationary. However, if $\alpha \ll 1/T$, the log-volatility behaves locally (at time scales smaller than T) as a fBm. This observation is formalized in the following proposition.

Proposition 3.1. *Let W^H be a fBm and X^α defined by* (3.3) *for a given $\alpha > 0$. As α tends to zero,*

$$\mathbb{E}\Big[\sup_{t \in [0,T]} |X_t^\alpha - X_0^\alpha - \nu W_t^H|\Big] \to 0.$$

The proof is given in Appendix A.1.

Proposition 3.1 implies that in the RFSV model, if $\alpha \ll 1/T$, and we confine ourselves to the interval $[0, T]$, we can proceed as if the the log-volatility process were a fBm. Indeed, simply setting $\alpha = 0$ in (3.3) gives (at least formally) $X_t - X_s = \nu(W_t^H - W_s^H)$ and we immediately recover our simple non-stationary fBm model (3.1). Consequently, although the RFSV model is technically stationary, its ergodic behavior is of no interest for us; for example, estimation of the mean of the volatility is not possible in practice.

Indeed, at any time scale of practical interest (from one day to several years), we see no evidence of ergodicity in the data, see Figure 3.4.

The following corollary implies that the (exact) scaling property of the fBm is approximately reproduced by the fractional Ornstein-Uhlenbeck process when α is small.

Corollary 3.1. *Let $q > 0,\ t > 0,\ \Delta > 0$. As α tends to zero, we have*

$$\mathbb{E}[|X^\alpha_{t+\Delta} - X^\alpha_t|^q] \to \nu^q \, K_q \, \Delta^{qH}.$$

The proof is given in Appendix A.2.

RFSV versus FSV

We recognize our RFSV model (3.4) as a particular case of the classical FSV model of Comte and Renault [21]. The key difference is that here we take $H < 1/2$ and $\alpha \ll 1/T$, whereas to accommodate the assumption of long memory, Comte and Renault have to choose $H > 1/2$. The analysis of Fukasawa referred to earlier in Section 1.3 implies in particular that if $H > 1/2$, the volatility skew function $\psi(\tau)$ is *increasing* in time to expiration τ (at least for small τ), which is obviously completely inconsistent with the approximately $1/\sqrt{\tau}$ skew term structure that is observed. To generate a decreasing term structure of volatility skew for longer expirations, Comte and Renault are then forced to choose $\alpha \gg 1/T$. Consequently, for very short expirations ($\tau \ll 1/\alpha$), models of the Comte and Renault type with $H > 1/2$ still generate a term structure of volatility skew that is inconsistent with the observed one, as explained for example in Section 4 of [20].

In contrast, the choice $H < 1/2$ enables us to reproduce the observed smoothness and scaling of the volatility process and generate a term structure of volatility skew in agreement with the observed one. The choice $H < 1/2$ is also consistent with what is improperly called mean reversion by practitioners, which in fact corresponds to strong oscillations in the volatility process. Finally, taking α very small implies that the dynamics of our process is close to that of a fBm, see Proposition 3.1. This last point is particularly important. Indeed, recall that at the time scales we are interested in, the important feature we have in mind is really this fBm like-behavior of the log-volatility.

Finally, note that we could no doubt have considered other stationary models satisfying Proposition 3.1 and Corollary 3.1, where log-volatility behaves as a fBm at reasonable time scales; the choice of the fractional Ornstein-Uhlenbeck process is probably the simplest way to accommodate this local behavior together with the stationarity property.

3.2 RFSV model autocovariance functions

From Proposition 3.1 and Corollary 3.1, we easily deduce the following corollary, where $o(1)$ tends to zero as α tends to zero.

Corollary 3.2. *Let $q > 0,\ t > 0,\ \Delta > 0$. As α tends to zero,*

$$\mathrm{Cov}[X_t^\alpha, X_{t+\Delta}^\alpha] = \mathrm{Var}[X_t^\alpha] - \frac{1}{2}\,\nu^2\,\Delta^{2H} + o(1).$$

Consequently, in the RFSV model, for fixed t, the covariance between X_t and $X_{t+\Delta}$ is linear with respect to Δ^{2H}. This result is very well satisfied empirically. For example, in Figure 3.1, we see that for the S&P, the empirical autocovariance function of the log-volatility is indeed linear with respect to Δ^{2H}. Note in passing that at the time scales we consider, the term $\mathrm{Var}[X_t^\alpha]$ is higher than $\frac{1}{2}\nu^2\,\Delta^{2H}$ in the expression for $\mathrm{Cov}[X_t^\alpha, X_{t+\Delta}^\alpha]$.

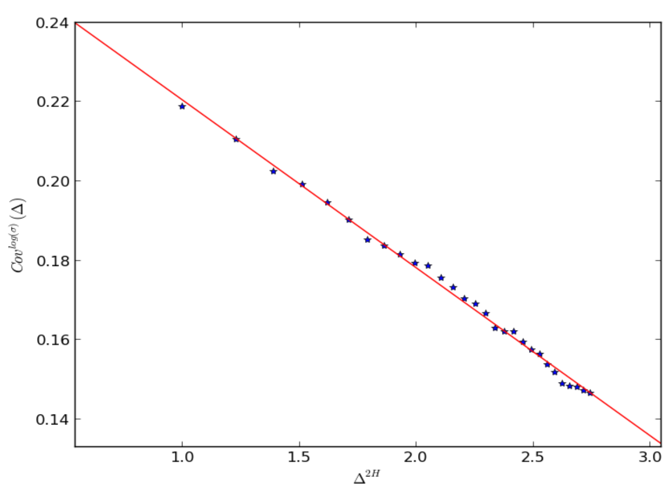

Figure 3.1: Autocovariance of the log-volatility as a function of Δ^{2H} for $H = 0.14$, S&P.

Having computed the autocovariance function of the log-volatility, we now turn our attention to the volatility itself. We have

$$\mathbb{E}[\sigma_{t+\Delta}\sigma_t] = \mathbb{E}[e^{X_t^\alpha + X_{t+\Delta}^\alpha}],$$

with X^α defined by Equation (3.3). Since X^α is a Gaussian process, we deduce that

$$\mathbb{E}[\sigma_{t+\Delta}\sigma_t] = e^{\mathbb{E}[X_t^\alpha]+\mathbb{E}[X_{t+\Delta}^\alpha]+\mathrm{Var}[X_t^\alpha]/2+\mathrm{Var}[X_{t+\Delta}^\alpha]/2+\mathrm{Cov}[X_t^\alpha,X_{t+\Delta}^\alpha]}.$$

Applying Corollary 3.2, we obtain that when α is small, $\mathbb{E}[\sigma_{t+\Delta}\sigma_t]$ is approximately equal to

$$e^{2\mathbb{E}[X_t^\alpha]+2\mathrm{Var}[X_t^\alpha]}e^{-\nu^2\frac{\Delta^{2H}}{2}}. \tag{3.5}$$

It follows that in the RFSV model, $\log(\mathbb{E}[\sigma_{t+\Delta}\sigma_t])$ is also linear in Δ^{2H}. This property is again very well satisfied on data, as shown by Figure 3.2, where we plot the logarithm of the empirical counterpart of $\mathbb{E}[\sigma_{t+\Delta}\sigma_t]$ against Δ^{2H}, for the S&P with $H = 0.14$.

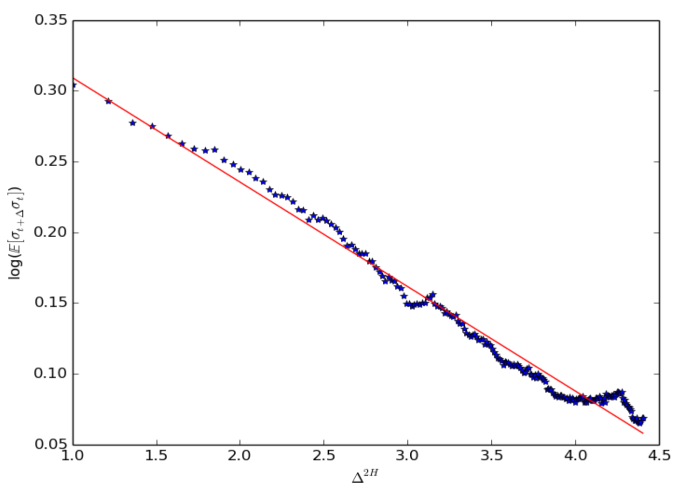

Figure 3.2: Empirical counterpart of $\log(\mathbb{E}[\sigma_{t+\Delta}\sigma_t])$ as a function of Δ^{2H}, S&P.

We note that putting Δ^{2H} on the x-axis of Figure 3.2 is really crucial in order to retrieve linearity. In particular, a corollary of (3.5) is that the autocovariance function of the volatility does not decay as a power law as widely believed; see Figure 3.3 where we show that a log-log plot of the autocovariance function does not yield a straight line.

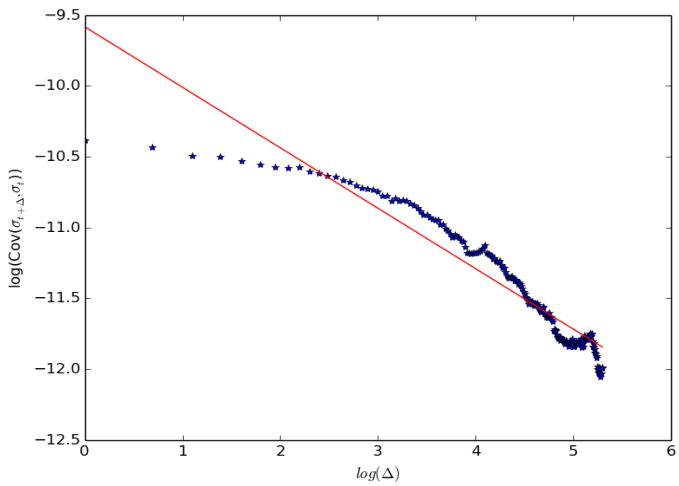

Figure 3.3: Empirical counterpart of $\log(\mathrm{Cov}[\sigma_{t+\Delta}, \sigma_t])$ as a function of $\log(\Delta)$, S&P.

3.3 RFSV versus FSV again

To further demonstrate the incompatibility of the classical long memory FSV model with volatility data, consider the quantity $m(2, \Delta)$. Recall that in the data (see Section 2) we observe the linear relationship $\log m(2, \Delta) \approx \zeta_2 \log \Delta + k$ for some constant k. Also, in both FSV and RFSV, we can consider

$$\begin{aligned} m(2,\Delta) &= \mathbb{E}\left[(X_{t+\Delta} - X_t)^2\right] \\ &= 2\left(\mathrm{Var}[X_t] - \mathrm{Cov}[X_t, X_{t+\Delta}]\right). \end{aligned}$$

In Figure 3.4, we plot $m(2, \Delta)$ with the parameters $H = 0.53$, corresponding to the FSV model parameter estimate of Chronopoulou and Viens in [18], and $\alpha = 0.5$ to ensure some visible decay of the volatility skew. The slope of $m(2, \Delta)$ in the FSV model for small lags is driven by the value of H; the lag at which $m(2, \Delta)$ begins to flatten and stationarity kicks in corresponds to a time scale of order $1/\alpha$. It is clear from the picture that to fit the data, we must have $\alpha \ll 1/T$ and the value of H must be set by the initial slope of the regression line, which as reported earlier in Section 2 is $\zeta_2 = 2 \times 0.14$.

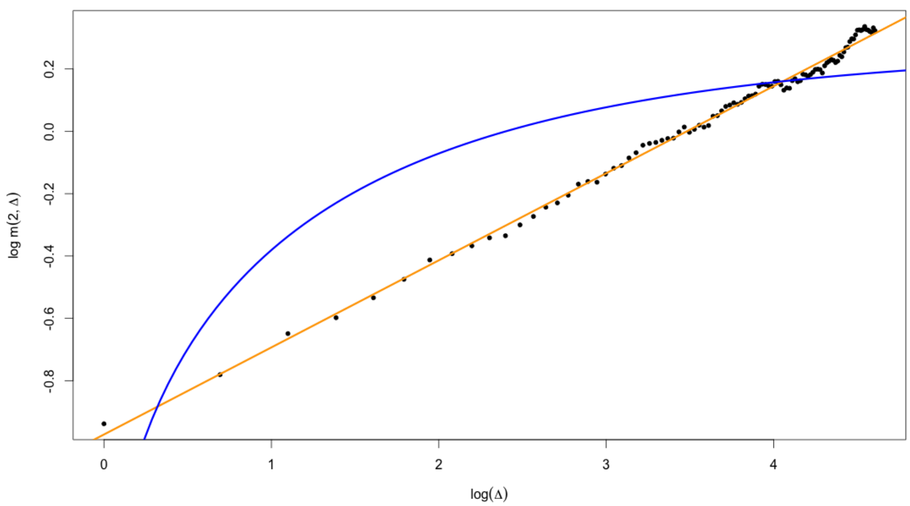

Figure 3.4: Long memory models such as the FSV model of Comte and Renault are not compatible with S&P volatility data. Black points are empirical estimates of $m(2, \Delta)$; the blue line is the FSV model with $\alpha = 0.5$ and $H = 0.53$; the orange line is the RFSV model with $\alpha = 0$ and $H = 0.14$.

3.4 Simulation-based analysis of the RFSV model

Our goal in this section is to show that in terms of smoothness measures, one obtains on simulated data from the RFSV model the same behaviors as those observed on empirical data. In particular, we would like to be able to quantify the positive bias associated with estimating H from whole-day realized variance data as in Section 2.3, relative to using data from a one-hour window as in Section 2.2.

We simulate the RFSV model for $2,000$ days (chosen to be between the lengths of our two datasets). In order to account for the overnight effect, we simulate the volatility σ_t[8] and efficient price P_t[9] over the whole day. The parameters: $H = 0.14$, $\nu = 0.3$, $m = X_0 = -5$ and $\alpha = 5 \times 10^{-4}$, are chosen to be consistent with our empirical estimates from Section 2. To model microstructure effects such as the discreteness of the price grid, we consider that the observed price process is generated from P_t using the uncertainty zones model of [49] with tick value 5×10^{-4} and parameter $\eta = 0.25$.

Exactly as in Section 2, for each of the 2,000 days, we consider two volatility proxies obtained from the observed price and based on:

- The integrated variance estimator using the model with uncertainty zones over one hour windows, from 10 am to 11 am.
- The 5 minutes realized variance estimator, over eight hours windows (the trading day).

We now repeat our analysis of Section 2, generating graphs analogous to Figures 2.1, 2.2, 2.4 and 2.5 obtained on empirical data. Figure 3.5 compares smoothness measures obtained using the uncertainty zones estimator on one-hour windows with those obtained using the realized variance estimator on 8-hour windows.

[8] To simulate the fBm, we use a spectral method with 40,000,000 points (20,000 points per day). We then simulate X taking $X_{(n+1)\delta} - X_{n\delta} = \nu(W^H_{(n+1)\delta} - W^H_{n\delta}) + \alpha\delta(m - X_{n\delta})$ (with $\delta = 1/20000$).

[9] $P_{(n+1)\delta} - P_{n\delta} = P_{n\delta}\sigma_{n\delta}\sqrt{\delta}\, U_n$ where the U_n are iid standard Gaussian variables.

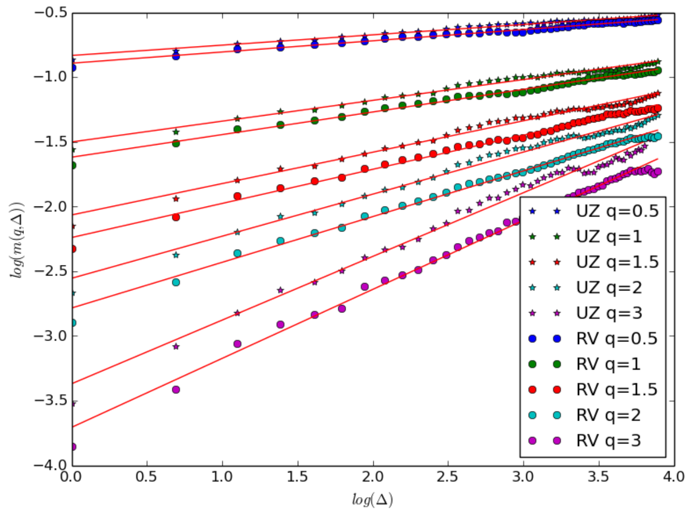

Figure 3.5: $\log(m(q, \Delta))$ as a function of $\log(\Delta)$, simulated data, with realized variance and uncertainty zones estimators.

When the uncertainty zones estimator is applied on a one-hour window (1/24 of a simulated day) as in Section 2.2, we estimate $H = 0.16$, which is close to the true value $H = 0.14$ used in the simulation. The results obtained with the realized variance estimator over daily eight-hour windows (1/3 of a simulated day) do exhibit the same scaling properties as those we see in the empirical data with a smoothness parameter that does not depend on q. However, the estimated H is biased slightly higher at around 0.18. As discussed in Section 2.1, this extra positive bias is no surprise and is due to the regularizing effect of the integral operator over the longer window. We note also that the estimated values of ν ("volatility of volatility" in some sense), obtained from the intercepts of the regressions, are lower with the longer time windows, again as expected. A detailed computation of the bias in the estimated H associated with the choice of window length in an analogous but more tractable model is presented in Appendix C.

We end this section by presenting in Figure 3.6 a sample path of the model-generated volatility (spot volatility, directly from the simulation rather than estimated from the simulated price series) together with a graph of S&P

volatility over $3,500$ days.

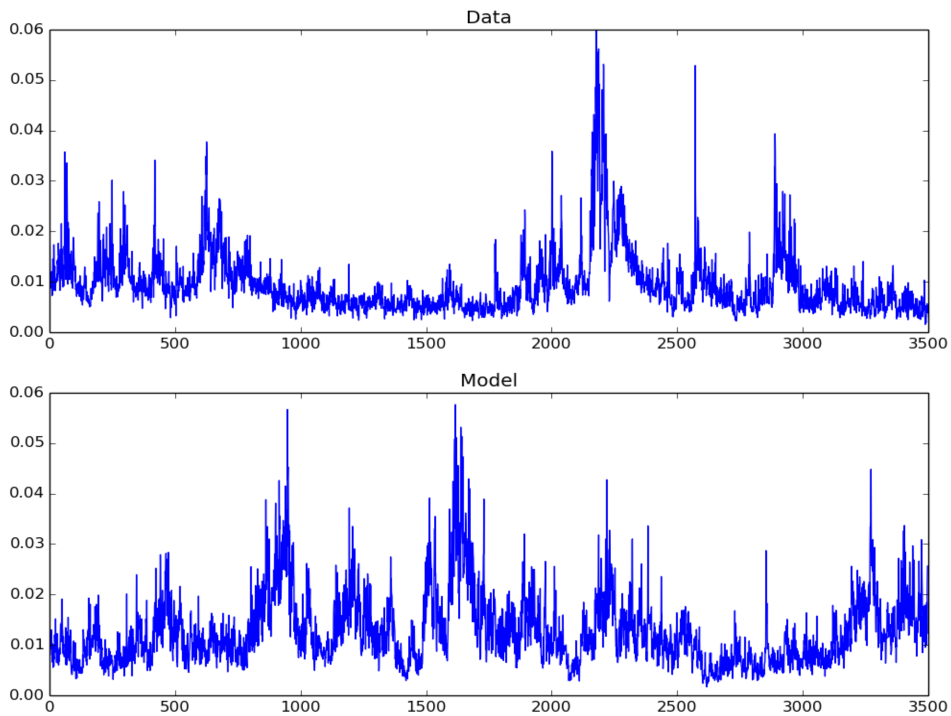

Figure 3.6: Volatility of the S&P (above) and generated by the model (below).

A first reaction to Figure 3.6 is that the simulated and actual graphs look very alike. In particular, in both of them, persistent periods of high volatility alternate with low volatility periods. On closer inspection of the empirical volatility series, we observe that the sample path of the volatility on a restricted time window seems to exhibit the same kind of qualitative properties as those of the global sample path (for example periods of high and low activity). This fractal-type behavior of the volatility has been investigated both empirically and theoretically in, for example, [6, 12, 44].

At the visual level, we observe that this fractal-type behavior is also reproduced in our model, as we now explain. Denote by $L^{x,H}$ the law of the geometric fractional Brownian motion with Hurst exponent H and volatility x on $[0,1]$, that is $(e^{xW_t^H})_{t\in[0,1]}$. Then, when α is very small, the rescaled volatility process on $[0,\Delta]$: $(\sigma_{t\Delta}/\sigma_0)_{t\in[0,1]}$, has approximately the law $L^{\nu\Delta^H,H}$. Now remark that for H small, the function u^H increases very slowly. Thus, over a large range of observation scales Δ, the rescaled volatility processes on $[0,\Delta]$ have approximately the same law. For example, between an observation scale of one day and five years (1250 open days), the coefficient x characterizing the law of the volatility process is "only" multiplied by $1250^{0.14} = 2.7$. It follows that in the RFSV model, the volatility process over one day resembles the volatility process over a decade.

4 Spurious long memory of volatility?

We revisit in this section the issue of long memory of volatility through the lens of our model. Recall that a stationary time series is said to exhibit long memory if the autocovariance function $\text{Cov}[\log(\sigma_t), \log(\sigma_{t+\Delta})]$ (or sometimes $\text{Cov}[\sigma_t, \sigma_{t+\Delta}]$) goes slowly to zero as $\Delta \to \infty$, and often even more precisely that it behaves as $\Delta^{-\gamma}$[10], with $\gamma < 1$ as $\Delta \to \infty$.

Thus, the classical approach to long memory is to consider a parametric class of models and to estimate within this class the parameter γ, typically based on empirical autocovariances, see [5] and Figure 3.3. As mentioned earlier in the introduction, the long memory of volatility is widely accepted as a stylized fact.

Specifically, in the RFSV model, we have from Corollary 3.2 that

$$\text{Cov}[\log(\sigma_t), \log(\sigma_{t+\Delta})] \approx A - B\Delta^{2H}$$

and from Equation (3.5) that

$$\text{Cov}[\sigma_t, \sigma_{t+\Delta}] \approx C\, e^{-B\Delta^{2H}} - D,$$

[10]Indeed the notion of empirical long memory does not make much sense outside the power law case; the empirical values of covariances at very large time scales are never measurable and thus one cannot conclude whether the series of covariances converges in general.

for some constants A, B, C and D. Moreover, we demonstrated in Figures 3.1 and 3.2 that these relations are consistent with the data. Thus the autocovariance function does not decay as a power law in the RFSV model nor does it appear to decay as a power law in the data.

Nevertheless, as an experiment, we can apply both to the data and to sample paths of the RFSV model some standard statistical procedures aimed at identifying long memory that have been used in the financial econometrics literature. Such procedures are of course designed to identify long memory under rather strict modeling assumptions. Consequently, spurious results may obviously then be obtained if the model underlying the estimation procedure is misspecified, which is the case with the RFSV model[11].

With the same model parameters as in Section 3.4, we simulate our model over 3,500 days, which corresponds to the size of our dataset. Consider first the procedure in [4], where in the context of a fractional Gaussian noise (FGN) model with Hurst parameter $\hat{H}$, the authors test for long memory in the volatility by studying the scaling behavior of the quantity

$$V(\Delta) = \mathrm{Var}\left[\int_0^\Delta \sigma_s^2 ds\right]$$

with respect to Δ. In the FGN model, as $\Delta \to \infty$, the autocorrelation function $\rho(\Delta)$ behaves asymptotically as $\Delta^{2\hat{H}-2}$ and $V(\Delta)$ behaves asymptotically as $\Delta^{2\hat{H}}$ as $\Delta \to \infty$. Figure 4.1 presents the graph of the logarithm of the empirical counterpart of $V(\Delta)$ against the logarithm of Δ, on the S&P data and within our simulation framework.

[11] Recall in particular that the RFSV model is only formally stationary.

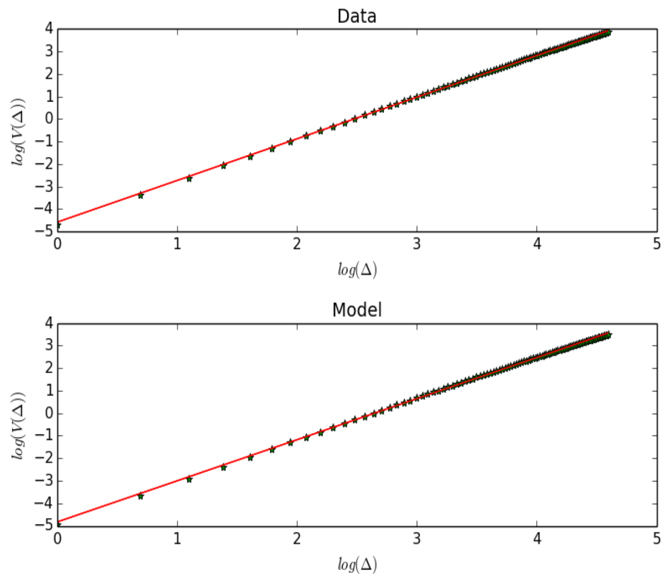

Figure 4.1: Empirical counterpart of $\log(V(\Delta))$ as a function of $\log(\Delta)$ on S&P (above) and simulation (below).

We note from Figure 4.1 that both our simulated model and market data lead to very similar graphs, close to straight lines with slope 1.86, giving $\hat{H} = 0.93$[12]. Accordingly, in the setting of [4], we would deduce power law behavior of the autocorrelation function with exponent 0.14 and therefore long memory. Thus, if the data are generated by a model like the RFSV model, one can easily be wrongly convinced that the volatility time series exhibits long memory.

In [5], in the context of an ARFIMA$(0, d, 0)$ model, the authors deduce long memory in the volatility by showing that the process ε_t obtained by fractional differentiation of the log-volatility $\varepsilon_t = (1 - L)^d \log(\sigma_t)$, with $d = 0.401$[13](which is obtained by regression of the log-periodogram using the GPH estimator [36]) and L the lag operator, behaves as a white noise. To

[12]Note that there is no reason to expect that there should be any direct connection between $\hat{H}$ estimated for the FGN model and the H we estimated for the RFSV model.

[13]It is shown in [36] that the autocorrelation functions of the ARFIMA$(0, d, 0)$ and the FGN model with Hurst parameter $\hat{H}$ have the same asymptotic behavior as $\Delta \to \infty$ if $d = \hat{H} - \frac{1}{2}$.

check for this, they compute the autocorrelation function of ε_t. We give in Figure 4.2 the autocorrelation functions of the logarithm of σ_t and ε_t, again both on the data and on the simulated path.

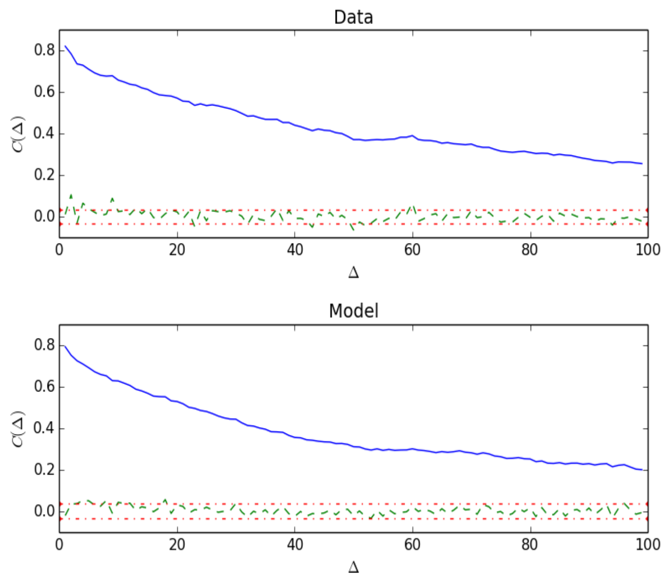

Figure 4.2: Autocorrelation functions of $\log(\sigma_t)$ (in blue) and ε_t (in green) and the Bartlett standard error bands (in red), for S&P data (above) and for simulated data (below).

Once again, the data and the simulation generate very similar plots. We conclude that this procedure for estimating long memory is just as fragile as the first, and it is easy to wrongly deduce volatility long memory when applying it.

In conclusion, the RFSV model is yet another model in which classical estimation procedures identify spurious long memory; see [1, 25, 37, 38] for various other such examples. Moreover, these procedures estimate the same long memory parameter from data generated from a suitably calibrated RFSV model as they estimate from empirical data. Once again, although the (near) non-stationarity of the RFSV model induces long swings in volatility, mirroring long-range dependence, it does not exhibit long memory in the classical power law sense.

5 Forecasting using the RFSV model

In this section, we present an application of our model: forecasting the log-volatility and the variance.

5.1 Forecasting log-volatility

The key formula on which our prediction method is based is the following one:

$$\mathbb{E}[W^H_{t+\Delta}|\mathcal{F}_t] = \frac{\cos(H\pi)}{\pi}\Delta^{H+1/2}\int_{-\infty}^{t}\frac{W^H_s}{(t-s+\Delta)(t-s)^{H+1/2}}ds,$$

where W^H is a fBm with $H < 1/2$ and $\mathcal{F}_t$ the filtration it generates, see Theorem 4.2 of [48]. By construction, over any reasonable time scale of interest, as formalized in Corollary 3.1, we may approximate the fractional Ornstein-Uhlenbeck volatility process in the RFSV model as $\log\sigma_t^2 \approx 2\nu\, W^H_t + C$, for some constants ν and C. Our prediction formula for log-variance then follows:[14]

$$\mathbb{E}\left[\log\sigma^2_{t+\Delta}|\mathcal{F}_t\right] = \frac{\cos(H\pi)}{\pi}\Delta^{H+1/2}\int_{-\infty}^{t}\frac{\log\sigma^2_s}{(t-s+\Delta)(t-s)^{H+1/2}}ds. \quad (5.1)$$

This formula, or rather its approximation through a Riemann sum (we assume in this section that the volatilities are perfectly observed, although they are in fact estimated), is used to forecast the log-volatility 1, 5 and 20 days ahead ($\Delta = 1,\ 5,\ 20$).

We now compare the predictive power of Formula (5.1) with that of autoregressive (AR for short) and heterogeneous autoregressive (HAR for short) forecasts, in the spirit of [23][15]. Recall that for a given integer $p > 0$, the AR(p) and HAR predictors take the following form (where the index i runs over the series of daily volatility estimates):

[14]The constants 2ν and C cancel when deriving the expression.

[15] Note that we do not consider GARCH models here since we have access to high frequency volatility estimates and not only to daily returns. Indeed, it is shown in [5] that forecasts based on the time series of realized variances outperform GARCH forecasts based on daily returns.

- AR(p):

$$\widehat{\log(\sigma^2_{t+\Delta})} = K_0^\Delta + \sum_{i=0}^{p} C_i^\Delta \log(\sigma^2_{t-i}).$$

- HAR :

$$\widehat{\log(\sigma^2_{t+\Delta})} = K_0^\Delta + C_0^\Delta \log(\sigma^2_t) + C_5^\Delta \frac{1}{5}\sum_{i=0}^{4} \log(\sigma^2_{t-i}) + C_{20}^\Delta \frac{1}{20}\sum_{i=0}^{19} \log(\sigma^2_{t-i}).$$

We estimate AR coefficients using the R `stats` library[16] on a rolling time window of 500 days. In the HAR case, we use standard linear regression to estimate the coefficients as explained in [23]. In the sequel, we consider $p = 5$ and $p = 10$ in the AR formula. Indeed, these parameters essentially give the best results for the horizons at which we wish to forecast the volatility (1, 5 and 20 days). For each day, we forecast volatility for five different indices[17].

We then assess the quality of the various forecasts by computing the ratio P between the mean squared error of our predictor and the (approximate) variance of the log-variance:

$$P = \frac{\sum_{k=500}^{N-\Delta} \left(\log(\sigma^2_{k+\Delta}) - \widehat{\log(\sigma^2_{k+\Delta})}\right)^2}{\sum_{k=500}^{N-\Delta} \left(\log(\sigma^2_{k+\Delta}) - \mathbb{E}[\log(\sigma^2_{t+\Delta})]\right)^2},$$

where $\mathbb{E}[\log(\sigma^2_{t+\Delta})]$ denotes the empirical mean of the log-variance over the whole time period.

[16]More precisely, we use the default Yule-Walker method.

[17]In addition to S&P and NASDAQ, we also investigate CAC40, FTSE and Nikkei, over the same time period as S&P and NASDAQ. For simplicity, the parameter H used in our predictor is computed only once for each asset, using the whole time period. This yields similar results to using a moving time window adapted in time.

	AR(5)	AR(10)	HAR(3)	RFSV
SPX2.rv $\Delta = 1$	0.317	0.318	0.314	**0.313**
SPX2.rv $\Delta = 5$	0.459	0.449	0.437	**0.426**
SPX2.rv $\Delta = 20$	0.764	0.694	0.656	**0.606**
FTSE2.rv $\Delta = 1$	0.230	0.229	0.225	**0.223**
FTSE2.rv $\Delta = 5$	0.357	0.344	0.337	**0.320**
FTSE2.rv $\Delta = 20$	0.651	0.571	0.541	**0.472**
N2252.rv $\Delta = 1$	0.357	0.358	0.351	**0.345**
N2252.rv $\Delta = 5$	0.553	0.533	0.513	**0.504**
N2252.rv $\Delta = 20$	0.875	0.795	0.746	**0.714**
GDAXI2.rv $\Delta = 1$	0.237	0.238	0.234	**0.231**
GDAXI2.rv $\Delta = 5$	0.372	0.362	0.350	**0.339**
GDAXI2.rv $\Delta = 20$	0.661	0.590	0.550	**0.498**
FCHI2.rv $\Delta = 1$	0.244	0.244	0.241	**0.238**
FCHI2.rv $\Delta = 5$	0.378	0.373	0.366	**0.350**
FCHI2.rv $\Delta = 20$	0.669	0.613	0.598	**0.522**

Table 5.1: Ratio P for the AR, HAR and RFSV predictors.

We note from Table 5.1 that the RFSV forecast consistently outperforms the AR and HAR forecasts, especially at longer horizons. Moreover, our forecasting method is more parsimonious since it only requires the parameter H to forecast the log-variance. Compare this with the AR and HAR methods, for which coefficients depend on the forecast time horizon and must be recomputed if this horizon changes.

Remark that our predictor can be linked to that of [27], where the issue of the prediction of the log-volatility in the multifractal random walk model of [6] is tackled. In this model,

$$\mathbb{E}[\log(\sigma^2_{t+\Delta})|\mathcal{F}_t] = \frac{1}{\pi}\sqrt{\Delta}\int_{-\infty}^{t} \frac{\log(\sigma^2_s)}{(t-s+\Delta)\sqrt{t-s}}ds,$$

which is the limit of our predictor when H tends to zero.

Note also that our prediction formula may be rewritten as

$$\mathbb{E}[\log(\sigma^2_{t+\Delta})|\mathcal{F}_t] = \frac{\cos(H\pi)}{\pi}\int_0^{+\infty} \frac{\log(\sigma^2_{t-\Delta u})}{(u+1)\,u^{H+1/2}}du.$$

For a given small $\varepsilon > 0$, let r be the smallest real number such that

$$\int_r^{+\infty} \frac{1}{(u+1)\, u^{H+1/2}} du \leq \varepsilon.$$

Then we have, with an error of order ε,

$$\mathbb{E}[\log(\sigma^2_{t+\Delta})|\mathcal{F}_t] \approx \frac{\cos(H\pi)}{\pi} \int_0^r \frac{\log(\sigma^2_{t-\Delta u})}{(u+1)\, u^{H+1/2}} du.$$

Consequently, the volatility process needs to be considered (roughly) down to time $t - \Delta\, r$ if one wants to forecast up to time Δ in the future. The relevant regression window is thus linear in the forecasting horizon. For example, for $r = 1$, $\varepsilon = 0.35$ which is not so unreasonable. In this case, as is well-known to practitioners, to predict log-volatility one week ahead, one should essentially look at the volatility over the last week. If trying to predict log-volatility one month ahead, one should look at the volatility over the last month.

5.2 Variance prediction

Recall that $\log \sigma_t^2 \approx 2\, \nu\, W_t^H + C$ for some constant C. In [48], it is shown that $W^H_{t+\Delta}$ is conditionally Gaussian with conditional variance

$$\mathrm{Var}[W^H_{t+\Delta}|\mathcal{F}_t] = c\, \Delta^{2H}$$

where

$$c = \frac{\Gamma(3/2 - H)}{\Gamma(H+1/2)\, \Gamma(2-2H)}.$$

Thus, we obtain the following form for the RFSV predictor of the variance:

$$\widehat{\sigma^2_{t+\Delta}} = \exp\left(\widehat{\log \sigma^2_{t+\Delta}} + 2\, c\, \nu^2 \Delta^{2\,H}\right) \tag{5.2}$$

where $\widehat{\log(\sigma^2_{t+\Delta})}$ is the predictor from Section 5.1 and ν^2 is estimated as the exponential of the intercept in the linear regression of $\log(m(2,\Delta))$ on $\log(\Delta)$.

As previously, we compare in Table 5.2 the performances of the RFSV forecast with those of AR and HAR forecasts (constructed on variance rather than log-variance this time).

	AR(5)	AR(10)	HAR(3)	RFSV
SPX2.rv $\Delta = 1$	0.520	0.566	0.489	**0.475**
SPX2.rv $\Delta = 5$	0.750	0.745	0.723	**0.672**
SPX2.rv $\Delta = 20$	1.070	1.010	1.036	**0.903**
FTSE2.rv $\Delta = 1$	0.612	0.621	0.582	**0.567**
FTSE2.rv $\Delta = 5$	0.797	0.770	0.756	**0.707**
FTSE2.rv $\Delta = 20$	1.046	0.984	0.935	**0.874**
N2252.rv $\Delta = 1$	0.554	0.579	**0.504**	0.505
N2252.rv $\Delta = 5$	0.857	0.807	0.761	**0.729**
N2252.rv $\Delta = 20$	1.097	1.046	1.011	**0.964**
GDAXI2.rv $\Delta = 1$	0.439	0.448	0.399	**0.386**
GDAXI2.rv $\Delta = 5$	0.675	0.650	0.616	**0.566**
GDAXI2.rv $\Delta = 20$	0.931	0.850	0.816	**0.746**
FCHI2.rv $\Delta = 1$	0.533	0.542	0.470	**0.465**
FCHI2.rv $\Delta = 5$	0.705	0.707	0.691	**0.631**
FCHI2.rv $\Delta = 20$	0.982	0.952	0.912	**0.828**

Table 5.2: Ratio P for the AR, HAR and RFSV predictors.

We find again that the RFSV forecast typically outperforms AR and HAR, although it is worth noting that the HAR forecast is already visibly superior to the AR forecast.

Since our working paper first appeared, much work has been done to estimate the roughness of volatility of other assets, notably by Bennedsen, Lunde and Pakkanen in [8]. In an analysis of E-mini S&P 500 futures data, at all timescales over 15 minutes, the out-of-sample forecasting performance of the estimator (5.2) is shown to be very similar to the performance of the other more highly parameterized estimators proposed. Interestingly, at daily and higher timescales, the simple estimator (5.2) is actually shown to outperform the more complicated estimators. It is also notable that rough volatility was confirmed for more than five thousand equities in [8]; we are not yet aware of any asset for which rough volatility has not been confirmed.

We emphasize that our point in this forecasting exercise is not to show that our rough volatility based approach is really superior to others. For example, we could have considered alternative competitors to the RFSV formula or refine the HAR procedure. We only wish to demonstrate that our forecast is probably at least as good as other predictors whilst being simpler, requiring only the estimation of H.

6 Conclusion

Using daily realized variance estimates as proxies for daily spot (squared) volatilities, we uncovered two startlingly simple regularities in the resulting time series. First we found that the distributions of increments of log-volatility are approximately Gaussian, consistent with many prior studies. Secondly, we established the monofractal scaling relationship

$$\mathbb{E}\left[|\log(\sigma_\Delta) - \log(\sigma_0)|^q\right] = K_q\, \nu^q\, \Delta^{q\,H}, \tag{6.1}$$

where H can be seen as a measure of smoothness characteristic of the underlying volatility process; typically, $0.06 < H < 0.2$. The simple scaling relationship (6.1) naturally suggests that log-volatility may be modeled using fractional Brownian motion.

The resulting Rough Fractional Stochastic Volatility (RFSV) model turns out to be formally almost identical to the FSV model of Comte and Renault [21], with one major difference: In the FSV model, $H > 1/2$ to ensure long memory whereas in the RFSV model $H < 1/2$, typically, $H \approx 0.1$. Moreover, in the FSV model, the mean reversion coefficient α has to be large compared to $1/T$ to ensure a decaying volatility skew; in the RFSV model, the volatility skew decays naturally just like the observed volatility skew, $\alpha \ll 1/T$ and indeed for time scales of practical interest, we may proceed as if α were exactly zero.

We further showed that applying standard test procedures to volatility time series simulated with the RFSV model would lead us to erroneously deduce the presence of long memory, with parameters similar to those found in prior studies. Despite that volatility in the RFSV model (or in the data) is not a long memory process, we can therefore explain why long memory of volatility is widely accepted as a stylized fact.

Thus the RFSV model is able to replicate the stylized facts of the time series, *i.e. Volatility is rough*. More precisely, we have shown that within a specific class of models (which we strongly argue to be relevant), empirical daily realized variance values are much more likely to be sampled from a rough volatility process than from a smooth process. Whether or not instantaneous variance is rough cannot of course be determined ultimately since instantaneous variance is latent and not observable; as mentioned in the introduction, it is not even clear that such an object exists independently of a specific model.

It is of course plausible that other models are compatible with many of our observations. In fact, there are probably many ways to design a process so that most of our empirical results are reproduced (for example estimation errors when estimating volatility can be quite significant for some models, leading to downward biases in the measurement of the smoothness). However, what we show here is that we cannot find any evidence against the RFSV model. In statistical terms, the null hypothesis that the data generating process of the volatility is a RFSV model cannot be rejected based on our analysis. Even more, it is likely that the RFSV model is simpler, more parsimonious and more tractable than any other such model. In particular we do not address the question of volatility jumps. Neither do we insist that there are no jumps in volatility. Rather, one of the main messages of our work is that our model is able to replicate the stylized facts of the time series without having to appeal to jumps, see [11] for another example where a continuous process can mimic the properties obtained from data generated by a process with jumps.

As an application of the RFSV model, we showed how to forecast volatility at various time scales, at least as well as when using Fulvio Corsi's impressive HAR estimator, but with only one parameter – H!

We focus in this work on the statistical properties of the RFSV model. In [7], the authors explore the implications of the RFSV model (written under the physical measure $\mathbb{P}$) for option pricing (under the pricing measure $\mathbb{Q}$). In particular, following Mandelbrot and Van Ness, the fBm that appears in the definition (3.4) of the RFSV model may be represented as a fractional integral of a standard Brownian motion as follows [43]:

$$W_t^H = \int_0^t \frac{dW_s}{(t-s)^\gamma} + \int_{-\infty}^0 \left[\frac{1}{(t-s)^\gamma} - \frac{1}{(-s)^\gamma}\right] dW_s, \tag{6.2}$$

with $\gamma = \frac{1}{2} - H$. The observed anticorrelation between price moves and volatility moves may then be modeled naturally by anticorrelating the Brownian motion W that drives the volatility process with the Brownian motion driving the price process. As already proved by Fukasawa [32], such a model with a small H reproduces the observed decay of at-the-money volatility skew with respect to time to expiry, asymptotically for short times. It is shown that an appropriate extension of Fukasawa's model, consistent with the RFSV model, fits the entire implied volatility surface remarkably well. In particular, this model accurately reproduces the extreme short dated smiles, with no jumps. Moreover, despite that it would seem from (6.2) that knowledge of the entire path $\{W_s : s < t\}$ of the Brownian motion would be required, it turns out that the statistics of this path necessary for option pricing are traded and thus easily observed. Remarkably, Heston-type formulas can also be obtained in the rough volatility framework, see [30, 31].

Finally, note that there are microstructural foundations to rough volatility models. Indeed, it is explained in [29] how rough volatility emerges as the scaling limit of a Hawkes process based description of the order flow in the context of high frequency trading and metaorder splitting.

Acknowledgments

We are very grateful to the referees of Econometrica, the Journal of the American Statistical Association, the Journal of Business and Economic Statistics, and Quantitative Finance whose careful reading and valuable comments have helped us improve substantially our presentation of this work. We also thank Masaaki Fukasawa for several interesting discussions.

A Proofs

A.1 Proof of Proposition 3.1

Starting from Equation (3.3) and applying integration by parts, we get

$$X_t^\alpha = \nu W_t^H - \int_{-\infty}^t \nu\alpha e^{-\alpha(t-s)} W_s^H ds + m.$$

Therefore,

$$(X_t^\alpha - X_0^\alpha) - \nu W_t^H = -\int_0^t \nu\alpha e^{-\alpha(t-s)} W_s^H ds - \int_{-\infty}^0 \nu\alpha(e^{-\alpha(t-s)} - e^{\alpha s}) W_s^H ds.$$

Consequently,

$$\sup_{t\in[0,T]} |(X_t^\alpha - X_0^\alpha) - \nu W_t^H| \leq \nu\alpha T \hat{W}_T^H + \int_{-\infty}^0 \nu\alpha(e^{\alpha s} - e^{-\alpha(T-s)}) \hat{W}_s^H ds,$$

where $\hat{W}_t^H = \sup_{s\in[0,t]} |W_s^H|$. Using the maximum inequality of [47], we get

$$\mathbb{E}\big[\sup_{t\in[0,T]} |(X_t^\alpha - X_0^\alpha) - \nu W_t^H|\big] \leq c\big(\nu\alpha T T^H + \int_{-\infty}^0 \nu\alpha(T\alpha e^{\alpha s})|s|^H ds\big),$$

with c some constant. The term on the right hand side is easily seen to go to zero as α tends to zero.

A.2 Proof of Corollary 3.1

We first recall Equation (2.2) in [16] which writes:

$$\mathrm{Cov}[X_{t+\Delta}^\alpha, X_t^\alpha] = K\int_{\mathbb{R}} e^{i\Delta x} \frac{|x|^{1-2H}}{\alpha^2 + x^2} dx,$$

with $K = \nu^2\Gamma(2H+1)\sin(\pi H)/(2\pi)$[18]. Now remark that

$$\mathbb{E}[(X_{t+\Delta}^\alpha - X_t^\alpha)^2] = 2\mathrm{Var}[X_t^\alpha] - 2\mathrm{Cov}[X_{t+\Delta}^\alpha, X_t^\alpha].$$

Therefore,

$$\mathbb{E}[(X_{t+\Delta}^\alpha - X_t^\alpha)^2] = 2K\int_{\mathbb{R}} (1 - e^{i\Delta x}) \frac{|x|^{1-2H}}{\alpha^2 + x^2} dx.$$

This implies that for fixed Δ, $\mathbb{E}[|X_{t+\Delta}^\alpha - X_t^\alpha|^2]$ is uniformly bounded by

$$2K\int_{\mathbb{R}} (1 - e^{i\Delta x}) \frac{|x|^{1-2H}}{x^2} dx.$$

Moreover, $X_{t+\Delta}^\alpha - X_t^\alpha$ is a Gaussian random variable and thus for every q, its moment of order $(q+1)$ is uniformly bounded (in α) so that the family $|X_{t+\Delta}^\alpha - X_t^\alpha|^q$ is uniformly integrable. Therefore, since by Proposition 3.1,

$$|X_{t+\Delta}^\alpha - X_t^\alpha|^q \to \nu^q |W_{t+\Delta}^H - W_t^H|^q, \text{ in law},$$

we get the convergence of the sequence of expectations.

[18] This covariance is real because it is the Fourier transform of an even function.

B Estimations of H

B.1 On different indices

Index	$\zeta_{0.5}/0.5$	ζ_1	$\zeta_{1.5}/1.5$	$\zeta_2/2$	$\zeta_3/3$
SPX2.rv	0.128	0.126	0.125	0.124	0.124
FTSE2.rv	0.132	0.132	0.132	0.131	0.127
N2252.rv	0.131	0.131	0.132	0.132	0.133
GDAXI2.rv	0.141	0.139	0.138	0.136	0.132
RUT2.rv	0.117	0.115	0.113	0.111	0.108
AORD2.rv	0.072	0.073	0.074	0.075	0.077
DJI2.rv	0.117	0.116	0.115	0.114	0.113
IXIC2.rv	0.131	0.133	0.134	0.135	0.137
FCHI2.rv	0.143	0.143	0.142	0.141	0.138
HSI2.rv	0.079	0.079	0.079	0.080	0.082
KS11.rv	0.133	0.133	0.134	0.134	0.132
AEX.rv	0.145	0.147	0.149	0.149	0.149
SSMI.rv	0.149	0.153	0.156	0.158	0.158
IBEX2.rv	0.138	0.138	0.137	0.136	0.133
NSEI.rv	0.119	0.117	0.114	0.111	0.102
MXX.rv	0.077	0.077	0.076	0.075	0.071
BVSP.rv	0.118	0.118	0.119	0.120	0.120
GSPTSE.rv	0.106	0.104	0.103	0.102	0.101
STOXX50E.rv	0.139	0.135	0.130	0.123	0.101
FTSTI.rv	0.111	0.112	0.113	0.113	0.112
FTSEMIB.rv	0.130	0.132	0.133	0.134	0.134

Table B.1: Estimates of ζ_q for all indices in the Oxford-Man dataset.

B.2 On different time intervals[19]

Index	H (first half)	H (second half)
SPX2.rk	0.115	0.158
FTSE2.rk	0.140	0.156
N2252.rk	0.083	0.134
GDAXI2.rk	0.154	0.168
RUT2.rk	0.098	0.149
AORD2.rk	0.059	0.114
DJI2.rk	0.123	0.151
IXIC2.rk	0.094	0.156
FCHI2.rk	0.140	0.146
HSI2.rk	0.072	0.129
KS11.rk	0.109	0.147
AEX.rk	0.168	0.151
SSMI.rk	0.206	0.183
IBEX2.rk	0.122	0.149
NSEI.rk	0.112	0.124
MXX.rk	0.068	0.118
BVSP.rk	0.074	0.134
GSPTSE.rk	0.075	0.147
STOXX50E.rk	0.138	0.132
FTSTI.rk	0.080	0.171
FTSEMIB.rk	0.133	0.140

Table B.2: Estimates of H over two different time intervals for all indices in the Oxford-Man dataset

C The effect of smoothing

Although we are really interested in the model

$$\log \sigma_{t+\Delta} - \log \sigma_t = \nu \left(W^H_{t+\Delta} - W^H_t \right),$$

consider the more tractable (fractional Stein and Stein or fSS) model:

$$v_{t+\Delta} - v_t = \alpha \left(W^H_{t+\Delta} - W^H_t \right),$$

[19]Note that we used realized kernel rather than realized variance estimates to generate Table B.2. Results obtained using different estimators are almost indistinguishable.

where $v_t = \sigma^2$. We cannot observe v_t but suppose we can proxy it by the average

$$\hat{v}_t^\delta = \frac{1}{\delta}\int_0^\delta v_u \, du.$$

We would, for example, like to estimate $m(2,\Delta) = \mathbb{E}\left[(v_{t+\Delta} - v_t)^2\right]$. However, we need to proxy spot variance with integrated variance so instead we have the estimate

$$\begin{aligned}
m^\delta(2,\Delta) &= \mathbb{E}\left[(\hat{v}_{t+\Delta}^\delta - \hat{v}_t^\delta)^2\right] \\
&= \frac{1}{\delta^2}\,\mathbb{E}\left[\left(\int_0^\delta (v_{u+\Delta} - v_u)\, du\right)^2\right] \\
&= \frac{\alpha^2}{\delta^2}\int_0^\delta\int_0^\delta \mathbb{E}\left[(W_{u+\Delta}^H - W_u^H)\,(W_{s+\Delta}^H - W_s^H)\right]\, du\, ds \\
&= \int_0^\delta\int_0^\delta \left(|u-s+\Delta|^{2H} - |u-s|^{2H}\right) du\, ds, \qquad \text{(C.1)}
\end{aligned}$$

where the last step uses that:

$$\mathbb{E}\left[W_u^H\, W_s^H\right] = \frac{1}{2}\left(u^{2H} + s^{2H} - |u-s|^{2H}\right),$$

and the symmetry of the integral.

We assume that the length δ of the smoothing window is less than one day so $\Delta > \delta$. Then easy computations give

$$\begin{aligned}
&\int_0^\delta\int_0^\delta |u-s+\Delta|^{2H}\, du\, ds \\
= \;& \frac{1}{2H+1}\,\frac{1}{2H+2}\left((\Delta+\delta)^{2H+2} - 2\,\Delta^{2H+2} + (\Delta-\delta)^{2H+2}\right)
\end{aligned}$$

and

$$\int_0^\delta\int_0^\delta |u-s|^{2H}\, du\, ds \;=\; \frac{2}{2H+1}\,\frac{1}{2H+2}\,\delta^{2H+2}.$$

Substituting back into (C.1) gives

$$\begin{aligned}
m^\delta(2,\Delta) &= \alpha^2\,\Delta^{2H}\,\frac{1}{2H+1}\,\frac{1}{2H+2}\,\frac{1}{\theta^2}\left((1+\theta)^{2H+2} - 2 - 2\,\theta^{2H+2} + (1-\theta)^{2H+2}\right) \\
&=: \alpha^2\,\Delta^{2H}\, f(\theta).
\end{aligned}$$

where $\theta = \delta/\Delta$.

Figure C.1 shows the effect of smoothing on the estimated variance in the fSS model. Keeping δ fixed, as Δ increases, $f(\theta) = f(\delta/\Delta)$ increases towards one. Thus, in a linear regression of $\log m^\delta(2, \Delta)$ against $\log \Delta$, we will obtain a higher effective H (from the higher slope) and a lower effective ("volatility of volatility") α, exactly as we observed in the RSFV model simulations in Section 3.4.

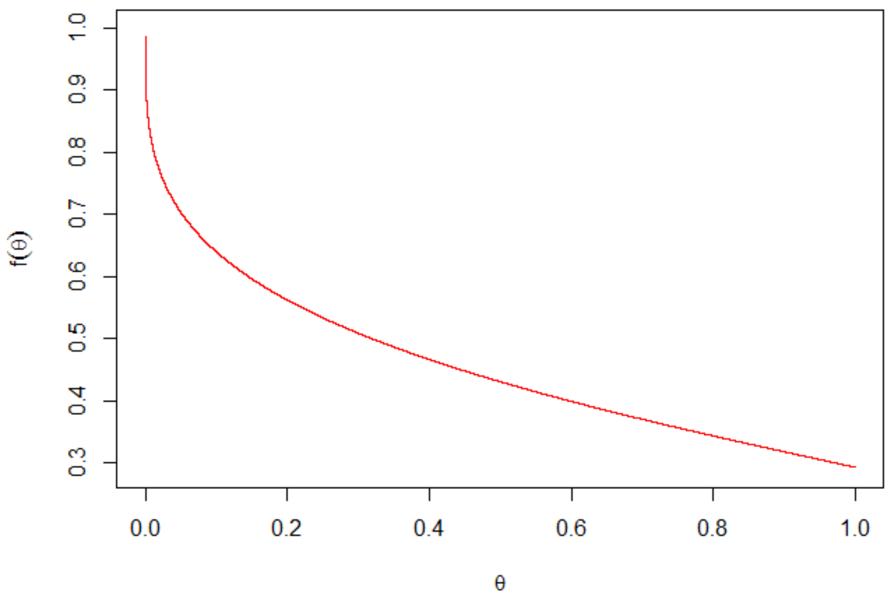

Figure C.1: $f(\theta)$ vs $\theta = \delta/\Delta$ with $H = 0.14$.

Numerical example

In the simulation of the RSFV model in Section 3.4, we have $H = 0.14$, $\delta_1 = 1/24$ for the UZ estimate and $\delta_2 = 1/3$ for the RV estimate. We now reproduce a fSS analogue of the RFSV simulation plots of $m(2, \Delta)$ in Figure 3.5. Specifically, for each $\Delta \in \{1, 2, ..., 100\}$, with $\alpha = 0.3$ and $\delta = \delta_1$ or

$\delta = \delta_2$, we compute the $m^\delta(2,\Delta)$ and regress $\log m^\delta(2,\Delta)$ against $\log\Delta$. The regressions are shown in Figure C.2 and results tabulated in Table C.1.

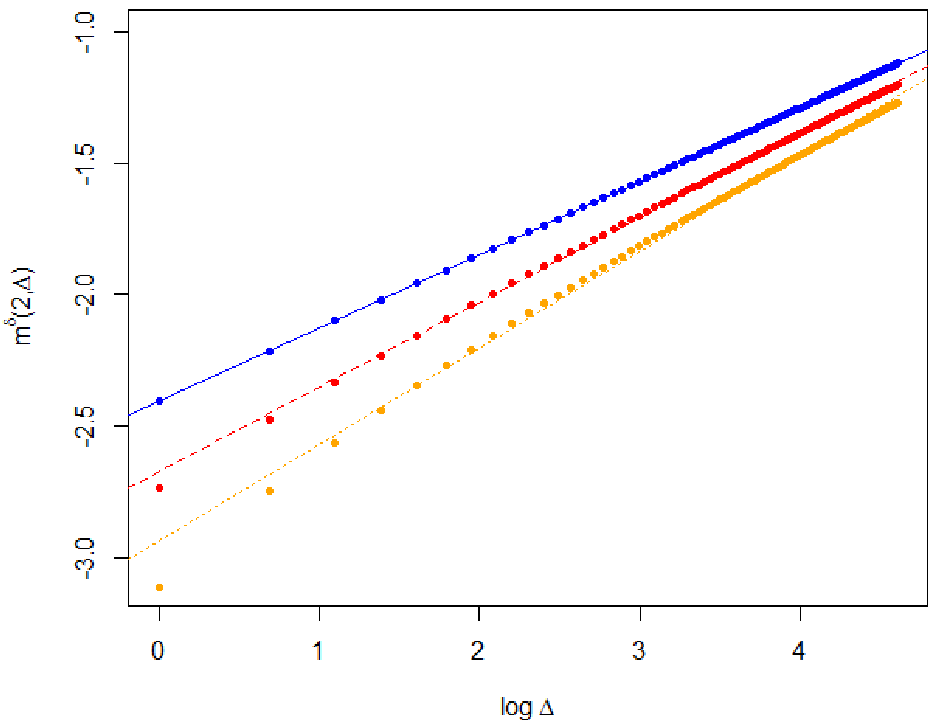

Figure C.2: Analogue of Figure 3.5 in the fSS model: The blue solid line is the true $m(2,\Delta)$; the red long-dashed line is the UZ estimate $m^{\delta_1}(2,\Delta)$; the orange short-dashed line is the RV estimate $m^{\delta_2}(2,\Delta)$.

In Figure C.2 and Table C.1, we observe similar qualitative and quantitative biases from our fSS model simulation as we observe in our simulation of the RSFV model with equivalent parameters in Section 3.4.

Estimate	Est. α	Est. H
Exact ($\delta = 0$)	0.300	0.140
UZ ($\delta = 1/24$)	0.263	0.161
RV ($\delta = 1/3$)	0.230	0.184

Table C.1: Estimated model parameters from the regressions shown in Figure C.2.

References

[1] T. G. Andersen and T. Bollerslev. Heterogeneous information arrivals and return volatility dynamics: Uncovering the long-run in high frequency returns. *The journal of Finance*, 52(3):975–1005, 1997.

[2] T. G. Andersen and T. Bollerslev. Intraday periodicity and volatility persistence in financial markets. *Journal of Empirical Finance*, 4(2):115–158, 1997.

[3] T. G. Andersen, T. Bollerslev, F. X. Diebold, and H. Ebens. The distribution of realized stock return volatility. *Journal of Financial Economics*, 61(1):43–76, 2001.

[4] T. G. Andersen, T. Bollerslev, F. X. Diebold, and P. Labys. The distribution of realized exchange rate volatility. *Journal of the American Statistical Association*, 96(453):42–55, 2001.

[5] T. G. Andersen, T. Bollerslev, F. X. Diebold, and P. Labys. Modeling and forecasting realized volatility. *Econometrica*, 71(2):579–625, 2003.

[6] E. Bacry and J. F. Muzy. Log-infinitely divisible multifractal processes. *Communications in Mathematical Physics*, 236(3):449–475, 2003.

[7] C. Bayer, P. Friz, and J. Gatheral. Pricing under rough volatility. *Quantitative Finance*, 16(6):887–904, 2016.

[8] M. Bennedsen, A. Lunde, and M. S. Pakkanen. Decoupling the short-and long-term behavior of stochastic volatility. *Available at SSRN 2846756*, 2016.

[9] S. R. Bentes and M. M. d. Cruz. Is stock market volatility persistent? a fractionally integrated approach. 2011.

[10] J. Beran. *Statistics for long-memory processes*, volume 61. CRC Press, 1994.

[11] B. M. Bibby, I. M. Skovgaard, M. Sørensen, et al. Diffusion-type models with given marginal distribution and autocorrelation function. *Bernoulli*, 11(2):191–220, 2005.

[12] J.-P. Bouchaud and M. Potters. *Theory of financial risk and derivative pricing: From statistical physics to risk management*. Cambridge University Press, 2003.

[13] A. Brouste and S. M. Iacus. Parameter estimation for the discretely observed fractional Ornstein–Uhlenbeck process and the Yuima R package. *Computational Statistics*, 28(4):1529–1547, 2013.

[14] P. Carr and L. Wu. What type of process underlies options? A simple robust test. *Journal of Finance*, 58(6):2581–2610, 2003.

[15] Z. Chen, R. T. Daigler, and A. M. Parhizgari. Persistence of volatility in futures markets. *Journal of Futures Markets*, 26(6):571–594, 2006.

[16] P. Cheridito, H. Kawaguchi, and M. Maejima. Fractional Ornstein-Uhlenbeck processes. *Electron. J. Probab*, 8(3):14, 2003.

[17] A. Chronopoulou. Parameter estimation and calibration for long-memory stochastic volatility models. In F. G. Viens, M. C. Mariani, and I. Florescu, editors, *Handbook of Modeling High-Frequency Data in Finance*, pages 219–231. John Wiley & Sons, 2011.

[18] A. Chronopoulou and F. G. Viens. Estimation and pricing under long-memory stochastic volatility. *Annals of Finance*, 8(2-3):379–403, 2012.

[19] J.-F. Coeurjolly. Estimating the parameters of a fractional Brownian motion by discrete variations of its sample paths. *Statistical Inference for Stochastic Processes*, 4(2):199–227, 2001.

[20] F. Comte, L. Coutin, and É. Renault. Affine fractional stochastic volatility models. *Annals of Finance*, 8(2-3):337–378, 2012.

[21] F. Comte and E. Renault. Long memory in continuous-time stochastic volatility models. *Mathematical Finance*, 8(4):291–323, 1998.

[22] R. Cont. Volatility clustering in financial markets: Empirical facts and agent-based models. In G. Teyssière and A. P. Kirman, editors, *Long Memory in Economics*, pages 289–309. Springer Berlin Heidelberg, 2007.

[23] F. Corsi. A simple approximate long-memory model of realized volatility. *Journal of Financial Econometrics*, 7(2):174–196, 2009.

[24] K. Dayri and M. Rosenbaum. Large tick assets: Implicit spread and optimal tick size. *Microtructure and Liquidity*, 1(1):155003, 2015.

[25] F. X. Diebold and A. Inoue. Long memory and regime switching. *Journal of econometrics*, 105(1):131–159, 2001.

[26] Z. Ding, C. W. Granger, and R. F. Engle. A long memory property of stock market returns and a new model. *Journal of Empirical Finance*, 1(1):83–106, 1993.

[27] J. Duchon, R. Robert, and V. Vargas. Forecasting volatility with the multifractal random walk model. *Mathematical Finance*, 22(1):83–108, 2012.

[28] B. Dupire. Pricing with a smile. *Risk Magazine*, 7(1):18–20, 1994.

[29] O. El Euch, M. Fukasawa, and M. Rosenbaum. The microstructural foundations of leverage effect and rough volatility. *arXiv preprint arXiv:1609.05177*, 2016.

[30] O. El Euch and M. Rosenbaum. The characteristic function of rough heston models. *arXiv preprint arXiv:1609.02108*, 2016.

[31] O. El Euch and M. Rosenbaum. Perfect hedging in rough heston models. *arXiv preprint arXiv:1703.05049*, 2017.

[32] M. Fukasawa. Asymptotic analysis for stochastic volatility: Martingale expansion. *Finance and Stochastics*, 15(4):635–654, 2011.

[33] J. Gatheral. *The volatility surface: A practitioner's guide*, volume 357. John Wiley & Sons, 2006.

[34] J. Gatheral and A. Jacquier. Arbitrage-free SVI volatility surfaces. *Quantitative Finance*, 14(1):59–71, 2014.

[35] J. Gatheral and R. C. Oomen. Zero-intelligence realized variance estimation. *Finance and Stochastics*, 14(2):249–283, 2010.

[36] J. Geweke and S. Porter-Hudak. The estimation and application of long memory time series models. *Journal of time series analysis*, 4(4):221–238, 1983.

[37] C. W. Granger and N. Hyung. Occasional structural breaks and long memory with an application to the s&p 500 absolute stock returns. *Journal of empirical finance*, 11(3):399–421, 2004.

[38] C. W. Granger and T. Teräsvirta. A simple nonlinear time series model with misleading linear properties. *Economics letters*, 62(2):161–165, 1999.

[39] P. S. Hagan, D. Kumar, A. S. Lesniewski, and D. E. Woodward. Managing smile risk. *Wilmott Magazine*, pages 84–108, 2002.

[40] S. L. Heston. A closed-form solution for options with stochastic volatility with applications to bond and currency options. *Review of Financial Studies*, 6(2):327–343, 1993.

[41] J. Hull and A. White. One-factor interest-rate models and the valuation of interest-rate derivative securities. *Journal of Financial and Quantitative Analysis*, 28(02):235–254, 1993.

[42] J. Istas and G. Lang. Quadratic variations and estimation of the local Hölder index of a Gaussian process. *Annales de l'IHP Probabilités et Statistiques*, 33(4):407–436, 1997.

[43] B. B. Mandelbrot and J. W. Van Ness. Fractional Brownian motions, fractional noises and applications. *SIAM review*, 10(4):422–437, 1968.

[44] R. N. Mantegna and H. E. Stanley. *Introduction to econophysics: Correlations and complexity in finance*. Cambridge University Press, 2000.

[45] T. Mikosch and C. Stărică. Is it really long memory we see in financial returns. In P. Embrechts, editor, *Extremes and integrated risk management*, pages 149–168. Risk Books, 2000.

[46] M. Musiela and M. Rutkowski. *Martingale methods in financial modelling*, volume 36. Springer, 2006.

[47] A. Novikov and E. Valkeila. On some maximal inequalities for fractional Brownian motions. *Statistics & Probability Letters*, 44(1):47–54, 1999.

[48] C. J. Nuzman and V. H. Poor. Linear estimation of self-similar processes via Lamperti's transformation. *Journal of Applied Probability*, 37(2):429–452, 2000.

[49] C. Y. Robert and M. Rosenbaum. A new approach for the dynamics of ultra-high-frequency data: The model with uncertainty zones. *Journal of Financial Econometrics*, 9(2):344–366, 2011.

[50] C. Y. Robert and M. Rosenbaum. Volatility and covariation estimation when microstructure noise and trading times are endogenous. *Mathematical Finance*, 22(1):133–164, 2012.

[51] M. Rosenbaum. Estimation of the volatility persistence in a discretely observed diffusion model. *Stochastic Processes and their Applications*, 118(8):1434–1462, 2008.

[52] M. Rosenbaum. First order p-variations and Besov spaces. *Statistics & Probability Letters*, 79(1):55–62, 2009.

[53] M. Rosenbaum. A new microstructure noise index. *Quantitative Finance*, 11(6):883–899, 2011.